Modular S_3 symmetric radiative seesaw model

Hiroshi Okada[1,2,*] and Yuta Orikasa[3,†]

[1]*Asia Pacific Center for Theoretical Physics, Pohang 37673, Republic of Korea*
[2]*Department of Physics, Pohang University of Science and Technology, Pohang 37673, Republic of Korea*
[3]*Institute of Experimental and Applied Physics, Czech Technical University in Prague, Husova 240/5, 110 00 Prague 1, Czech Republic*

(Received 31 July 2019; published 23 December 2019)

We propose a one-loop induced radiative seesaw model applying a modular S_3 flavor symmetry, which is known as the minimal non-Abelian discrete group. In this scenario, dark matter (DM) candidate is correlated with neutrinos and lepton flavor violations (LFVs). We show several predictions of mixings and phases satisfying LFVs, observed relic density, and neutrino oscillation data.

DOI: 10.1103/PhysRevD.100.115037

I. INTRODUCTION

Radiative seesaw models are one of the attractive scenarios to describe tiny neutrino masses and dark matter (DM) candidate at the same time [1]. Subsequently, several phenomenologies such as lepton flavor violations (LFVs), muon anomalous magnetic moment, and collider physics can be taken in account, depending on models. In addition, modular flavor symmetries have been recently proposed [2,3] to provide more predictions to the quark and lepton sector due to Yukawa couplings with a representation of a group. Their typical groups are found in basis of the A_4 modular group [3–18], S_3 [19–21], S_4 [15,17,22–28], A_5 [27,29,30], larger groups [31], multiple modular symmetries [32], and double covering of A_4 [33] in which masses, mixings, and CP phases for quark and lepton are predicted.[1] Furthermore, thanks to the modular weight that is another degree of freedom originated from modular symmetry, this modular weight can be identified as a symmetry to stabilize DM candidate if DM is included in a model. Thus, radiative seesaw models with modular flavor symmetries are well motivated in view of neutrino predictions and DM origin.

In this paper, we apply a S_3 modular symmetry to the lepton sector in a framework of Ma model [1], where S_3 is known as the minimal symmetry in non-Abelian discrete flavor symmetry. Here, we introduce two right-handed neutrinos that correspond to two singlets under S_3 and an isospin doublet inert boson in standard model (SM), both of which have nonzero charge of modular weight. In order to get a radiative seesaw model, we introduce additional Z_2 symmetry since the modular invariance is not sufficient to retain the radiative seesaw model. Therefore, Z_2 plays an role in assuring stability of DM. However, we realize a neutrino predictive model under one of the active neutrino masses is vanishing due to the two right-handed Majorana fermions, where the two kinds of fields originate from the fact that there are only two singlets under S_3.[2] This is the first achievement in several series of modular flavor symmetry projects.

In our analysis, we show several predictions to the lepton sector, satisfying constraints of LFVs as well as neutrino oscillation data. Also, bosonic DM is favored compared to the fermionic one, since the interacting coupling between DM and the SM particles are too tiny to explain the observed relic density.[3]

This paper is organized as follows. In Sec. II, we give our model set up under modular S_3 symmetry. Then, we discuss right-handed neutrino mass spectrum, lepton flavor violation (LFV), relic density of DM and generation of the active neutrino mass at one loop level. Finally we conclude and discuss in Sec. IV.

II. MODEL

The modular group $\bar{\Gamma}$ is the group of linear fractional transformation γ acting on the modulus τ, belonging to the upper-half complex plane as:

*hiroshi.okada@apctp.org
†Yuta.Orikasa@utef.cvut.cz

[1]Several reviews are helpful to understand whole the ideas [34–42] for traditional applications and [43,44] for modular symmetries.

[2]If we assign the right-handed Majorana fields as doublet under S_3, we cannot reproduce the observed neutrino oscillation data because of few free parameters.

[3]Another stabilization mechanism of DM candidate has been discussed in non-Abelian discrete symmetries in Refs. [45–47].

TABLE I. Field contents of fermions and bosons and their charge assignments under $SU(2)_L \times U(1)_Y \times S_3 \times Z_2$ in the lepton and boson sector, where $-k$ is the number of modular weight and the quark sector is the same as the SM.

	Fermions						Bosons	
	$\bar{L}_{L_e}$	$\bar{L}_{L_2} \equiv (\bar{L}_{L_\mu}, \bar{L}_{L_\tau})^T$	e_{R_e}	$e_{R_2} \equiv (e_{R_\mu}, e_{R_\tau})^T$	N_{R_1}	N_{R_2}	H	η^*
$SU(2)_L$	$\mathbf{2}$	$\mathbf{2}$	$\mathbf{1}$	$\mathbf{1}$	$\mathbf{1}$	$\mathbf{1}$	$\mathbf{2}$	$\mathbf{2}$
$U(1)_Y$	$\frac{1}{2}$	$\frac{1}{2}$	-1	-1	0	0	$\frac{1}{2}$	$-\frac{1}{2}$
S_3	1	2	1	2	1	$1'$	1	1
$-k$	-2	-2	-2	0	-2	-2	0	-2
Z_2	$+$	$+$	$+$	$+$	$-$	$-$	$+$	$-$

$$\tau \to \gamma\tau = \frac{a\tau + b}{c\tau + d}, \quad \text{where } a, b, c, d \in \mathbb{Z}$$
$$\text{and} \quad ad - bc = 1, \quad \mathrm{Im}[\tau] > 0, \tag{2.1}$$

which is isomorphic to $PSL(2,\mathbb{Z}) = SL(2,\mathbb{Z})/\{I, -I\}$ transformation. This modular transformation is generated by S and T,

$$S\colon\ \tau \to -\frac{1}{\tau}, \qquad T\colon\ \tau \to \tau + 1, \tag{2.2}$$

which satisfy the following algebraic relations,

$$S^2 = \mathbb{I}, \qquad (ST)^3 = \mathbb{I}. \tag{2.3}$$

We introduce the series of groups $\Gamma(N)(N = 1, 2, 3, \ldots)$ defined by

$$\Gamma(N) = \left\{ \begin{pmatrix} a & b \\ c & d \end{pmatrix} \in SL(2,\mathbb{Z}), \right. \\ \left. \times \begin{pmatrix} a & b \\ c & d \end{pmatrix} = \begin{pmatrix} 1 & 0 \\ 0 & 1 \end{pmatrix} (\mathrm{mod}\ N) \right\}. \tag{2.4}$$

For $N = 2$, we define $\bar{\Gamma}(2) \equiv \Gamma(2)/\{I, -I\}$. Since the element $-I$ does not belong to $\Gamma(N)$ for $N > 2$, we have $\bar{\Gamma}(N) = \Gamma(N)$, which are infinite normal subgroup of $\bar{\Gamma}$, called principal congruence subgroups. The quotient groups defined as $\Gamma_N \equiv \bar{\Gamma}/\bar{\Gamma}(N)$ are finite modular groups. In this finite groups Γ_N, $T^N = \mathbb{I}$ is imposed. The groups Γ_N with $N = 2$, 3, 4, 5 are isomorphic to S_3, A_4, S_4, and A_5, respectively [2].

Modular forms of level N are holomorphic functions $f(\tau)$ transforming under the action of $\Gamma(N)$ as:

$$f(\gamma\tau) = (c\tau + d)^k f(\tau), \qquad \gamma \in \Gamma(N), \tag{2.5}$$

where k is the so-called as the modular weight.

We discuss the modular symmetric theory without supersymmetry. In this paper, we fix the S_3 $(N = 2)$ modular group. Under the modular transformation of Eq. (2.1), fields $\phi^{(I)}$ transform as

$$\phi^{(I)} \to (c\tau + d)^{-k_I} \rho^{(I)}(\gamma)\phi^{(I)}, \tag{2.6}$$

where $-k_I$ is the modular weight and $\rho^{(I)}(\gamma)$ denotes an unitary representation matrix of $\gamma \in \Gamma(2)$.

The kinetic terms of their scalar fields are written by

$$\sum_I \frac{|\partial_\mu \phi^{(I)}|^2}{(-i\tau + i\bar{\tau})^{k_I}}, \tag{2.7}$$

which is invariant under the modular transformation. Also, the Lagrangian should be invariant under the modular symmetry.

Here, we describe our scenario based on the Ma model, where field contents are exactly the same as the Ma model [1]. The S_3 representation and modular weight are given by Table I, while the ones of Yukawa couplings are given by Table II. Under these symmetries, one writes renormalizable Lagrangian as follows:

$$\begin{aligned} -\mathcal{L}_{\mathrm{Lepton}} = {} & \alpha_\ell (Y_{\mathbf{2}}^{(2)} \otimes \bar{L}_{L_2} \otimes e_{R_2})_{\mathbf{1}} H + \beta_\ell (Y_{\mathbf{2}}^{(4)} \otimes \bar{L}_{L_2} \otimes e_{R_e})_{\mathbf{1}} H \\ & + \gamma_\ell (Y_{\mathbf{2}}^{(2)} \otimes \bar{L}_{L_e} \otimes e_{R_2})_{\mathbf{1}} H + \sigma_\ell (Y_{\mathbf{1}}^{(4)} \otimes \bar{L}_{L_e} \otimes e_{R_e})_{\mathbf{1}} H \\ & + \alpha_\nu (Y_{\mathbf{2}}^{(6)} \otimes \bar{L}_{L_2} \otimes N_{R_2})_{\mathbf{1}} \tilde{\eta} + \beta_\nu (Y_{\mathbf{1}'}^{(6)} \otimes \bar{L}_{L_e} \otimes N_{R_2})_{\mathbf{1}} \tilde{\eta} \\ & + \rho_\nu (Y_{\mathbf{1}}^{(6)} \otimes \bar{L}_{L_e} \otimes N_{R_1})_{\mathbf{1}} \tilde{\eta} + \sigma_\nu (Y_{\mathbf{2}}^{(6)} \otimes \bar{L}_{L_2} \otimes N_{R_1})_{\mathbf{1}} \tilde{\eta} \\ & + M_0 (Y_{\mathbf{1}}^{(4)} \otimes \bar{N}_{R_1}^C \otimes N_{R_1})_{\mathbf{1}} + M_1 (Y_{\mathbf{1}}^{(4)} \otimes \bar{N}_{R_2}^C \otimes N_{R_2})_{\mathbf{1}} + \mathrm{H.c.}, \end{aligned} \tag{2.8}$$

TABLE II. Modular weight assignments for Yukawa interaction.

	Couplings					
	$Y_{\mathbf{1}}^{(4)}$	$Y_{\mathbf{1}}^{(6)}$	$Y_{\mathbf{1'}}^{(6)}$	$Y_{\mathbf{2}}^{(2)}$	$Y_{\mathbf{2}}^{(4)}$	$Y_{\mathbf{2}}^{(6)}$
S_3	**1**	**1**	**1**	**2**	**2**	**2**
$-k$	4	6	6	2	4	6

where $\tilde{\eta} \equiv i\sigma_2\eta^*$, σ_2 being second Pauli matrix.

The modular forms with the lowest weight 2; $Y_{\mathbf{2}}^{(2)} \equiv (y_1, y_2)$, transforming as a doublet of S_3 is written in terms of Dedekind eta-function $\eta(\tau)$ and its derivative [48]:

$$y_1(\tau) = \frac{i}{4\pi}\left(\frac{\eta'(\tau/2)}{\eta(\tau/2)} + \frac{\eta'((\tau+1)/2)}{\eta((\tau+1)/2)} - \frac{8\eta'(2\tau)}{\eta(2\tau)}\right),$$
$$y_2(\tau) = \frac{\sqrt{3}i}{4\pi}\left(\frac{\eta'(\tau/2)}{\eta(\tau/2)} - \frac{\eta'((\tau+1)/2)}{\eta((\tau+1)/2)}\right). \tag{2.9}$$

Then, any couplings of higher weight are constructed by multiplication rules of S_3, and one finds the following couplings:

$$Y_{\mathbf{1}}^{(4)} = y_1^2 + y_2^2, \quad Y_{\mathbf{1}}^{(6)} = 3y_1^2 y_2 - y_2^3, \quad Y_{\mathbf{1'}}^{(6)} = y_1^3 - 3y_1 y_2^2,$$
$$Y_{\mathbf{2}}^{(4)} = \begin{bmatrix} 2y_1 y_2 \\ y_1^2 - y_2^2 \end{bmatrix}, \quad Y_{\mathbf{2}}^{(6)} = \begin{bmatrix} y_1^3 + y_1 y_2^2 \\ y_2^3 + y_1^2 y_2 \end{bmatrix}. \tag{2.10}$$

Higgs potential is given by

$$\mathcal{V} = -\mu_H^2 |H|^2 + \mu_\eta^2 |Y_{\mathbf{1}}^{(4)}||\eta|^2 + \frac{1}{4}\lambda_H |H|^4$$
$$+ \frac{1}{4}\lambda_\eta |Y_{\mathbf{1}}^{(8)}||\eta|^4 + \lambda_{H\eta}|Y_{\mathbf{1}}^{(4)}||H|^2|\eta|^2$$
$$+ \lambda'_{H\eta}|Y_{\mathbf{1}}^{(4)}||H^\dagger\eta|^2 + \frac{1}{4}\lambda''_{H\eta}[Y_{\mathbf{1}}^{(4)}(H^\dagger\eta)^2 + \text{H.c.}], \tag{2.11}$$

which can be the same as the original potential of Ma model without loss of generality, because of additional free parameters. The point is that one does not have a term $H^\dagger\eta$ due to absence of S_3 singlet with modular weight 2 that arises from the feature of modular symmetry.

The structure of Yukawa couplings are determined by the modular symmetry. Therefore, our model is more predictive than the standard Ma model. After the electroweak spontaneous symmetry breaking, the charged-lepton mass matrix is given by

$$m_\ell = \frac{v_H}{\sqrt{2}}\begin{bmatrix} \sigma_\ell Y_1^{(4)} & \gamma_\ell y_1 & \gamma_\ell y_2 \\ \beta_\ell(2y_1 y_2) & \alpha_\ell y_2 & \alpha_\ell y_1 \\ \beta_\ell(y_1^2 - y_2^2) & \alpha_\ell y_1 & -\alpha_\ell y_2 \end{bmatrix}, \tag{2.12}$$

where $\langle H\rangle \equiv [0, v_H/\sqrt{2}]^T$. Then the charged-lepton mass eigenstate can be found by $|D_\ell|^2 \equiv V_{e_L} m_\ell m_\ell^\dagger V_{e_L}^\dagger$. In our numerical analysis below, one can numerically fix the free parameters $\alpha_\ell, \beta_\ell, \gamma_\ell$ to fit the three charged-lepton masses after giving all the numerical values. Therefore, σ_ℓ is an input parameter that is free.

The right-handed neutrino mass matrix is given by

$$\mathcal{M}_N = \begin{bmatrix} M_0 Y_{\mathbf{1}}^{(4)} & 0 \\ 0 & M_1 Y_{\mathbf{1}}^{(4)} \end{bmatrix}. \tag{2.13}$$

It suggests that right-handed neutrinos are diagonal with two degenerate masses for the second and third fields, and we define $M_{N1} \equiv M_0 Y_{\mathbf{1}}^{(4)}$, $M_{N2} \equiv M_1 Y_{\mathbf{1}}^{(4)}$.

The Dirac Yukawa matrix is given by

$$y_D = \begin{bmatrix} \rho_\nu Y_{\mathbf{1}}^{(6)} & \beta_\nu Y_{\mathbf{1'}}^{(6)} \\ \sigma_\nu Y_{\mathbf{2,1}}^{(6)} & -\alpha_\nu Y_{\mathbf{2,2}}^{(6)} \\ \sigma_\nu Y_{\mathbf{2,2}}^{(6)} & \alpha_\nu Y_{\mathbf{2,1}}^{(6)} \end{bmatrix}, \tag{2.14}$$

where $Y_{\mathbf{2}}^{(6)} \equiv [Y_{\mathbf{2,1}}^{(6)}, Y_{\mathbf{2,2}}^{(6)}]^T$.

Lepton flavor violations also arises from y_D as [49,50]

$$\text{BR}(\ell_i \to \ell_j\gamma) \approx \frac{48\pi^3\alpha_{em}C_{ij}}{G_F^2(4\pi)^4}\left|\sum_{\alpha=1-3} y_{D_{j\alpha}} y_{D_{\alpha i}}^\dagger F(M_\alpha, m_{\eta^\pm})\right|^2, \tag{2.15}$$

$$F(m_a, m_b) \approx \frac{2m_a^6 + 3m_a^4 m_b^2 - 6m_a^2 m_b^4 + m_b^6 + 12m_a^4 m_b^2 \ln(\frac{m_b}{m_a})}{12(m_a^2 - m_b^2)^4}, \tag{2.16}$$

where $C_{21} = 1$, $C_{31} = 0.1784$, $C_{32} = 0.1736$, $\alpha_{em}(m_Z) = 1/128.9$, and $G_F = 1.166 \times 10^{-5}\ \text{GeV}^{-2}$. The experimental upper bounds are given by [51–53]

$$\text{BR}(\mu \to e\gamma) \lesssim 4.2 \times 10^{-13},$$
$$\text{BR}(\tau \to e\gamma) \lesssim 3.3 \times 10^{-8},$$
$$\text{BR}(\tau \to \mu\gamma) \lesssim 4.4 \times 10^{-8}, \tag{2.17}$$

which will be imposed in our numerical calculation.

Neutrino mass matrix is given at one-loop level by

$$m_{\nu_{ij}} \approx \sum_{\alpha=1,2} \frac{y_{D_{i\alpha}} M_{N\alpha} y_{D_{\alpha j}}^T}{(4\pi)^2}\left(\frac{m_R^2}{m_R^2 - M_{N\alpha}^2}\ln\left[\frac{m_R^2}{M_{N\alpha}^2}\right]\right.$$
$$\left. - \frac{m_I^2}{m_I^2 - M_{N\alpha}^2}\ln\left[\frac{m_I^2}{M_{N\alpha}^2}\right]\right), \tag{2.18}$$

where $m_{R(I)}$ is a mass of the real (imaginary) component of η^0. Then the neutrino mass matrix is diagonalized by an unitary matrix U_ν as $U_\nu m_\nu U_\nu^T = \text{diag}(m_{\nu_1}, m_{\nu_2}, m_{\nu_3}) \equiv D_\nu$, where $\text{Tr}[D_\nu] \lesssim 0.12$ eV is given by the recent cosmological data [54]. Then, one finds $U_{\rm PMNS} = V_{eL}^\dagger U_\nu$. Each of mixing is given in terms of the component of $U_{\rm MNS}$ as follows:

$$\sin^2\theta_{13} = |(U_{\rm PMNS})_{13}|^2, \quad \sin^2\theta_{23} = \frac{|(U_{\rm PMNS})_{23}|^2}{1-|(U_{\rm PMNS})_{13}|^2},$$
$$\sin^2\theta_{12} = \frac{|(U_{\rm PMNS})_{12}|^2}{1-|(U_{\rm PMNS})_{13}|^2}. \tag{2.19}$$

We provide the experimentally allowed ranges for neutrino mixings and mass difference squares at 3σ range [55] as follows:

$$\Delta m^2_{\rm atm} = [2.431 - 2.622] \times 10^{-3}\ {\rm eV}^2,$$
$$\Delta m^2_{\rm sol} = [6.79 - 8.01] \times 10^{-5}\ {\rm eV}^2,$$
$$\sin^2\theta_{13} = [0.02044 - 0.02437],$$
$$\sin^2\theta_{23} = [0.428 - 0.624],$$
$$\sin^2\theta_{12} = [0.275 - 0.350]. \tag{2.20}$$

Also, the effective mass for the neutrinoless double beta decay is given by

$$m_{ee} = |D_{\nu_1}\cos^2\theta_{12}\cos^2\theta_{13} + D_{\nu_2}\sin^2\theta_{12}\cos^2\theta_{13}e^{i\alpha_{21}} + D_{\nu_3}\sin^2\theta_{13}e^{i(\alpha_{31}-2\delta_{CP})}|, \tag{2.21}$$

where its observed value could be measured by KamLAND-Zen in future [56].

To achieve numerical analysis, we derive several relations of the normalized neutrino mass matrix as follows:

$$\tilde m_{\nu_{ij}} \equiv \frac{m_{\nu_{ij}}}{k_3} \approx \frac{1}{(4\pi)^2}\sum_{\alpha=1-3} y_{D_{i\alpha}}\tilde k_\alpha y^T_{D_{\alpha j}}, \qquad \tilde k_\alpha \equiv \frac{k_\alpha}{k_3},$$
$$k_\alpha \equiv M_{N\alpha}\left(\frac{m_R^2}{m_R^2 - M_{N\alpha}^2}\ln\left[\frac{m_R^2}{M_{N\alpha}^2}\right] - \frac{m_I^2}{m_I^2 - M_{N\alpha}^2}\ln\left[\frac{m_I^2}{M_{N\alpha}^2}\right]\right)$$
$$\approx M_{N\alpha}\Delta m^2\left(\frac{M_{N\alpha}^2 - m_R^2 + M_{N\alpha}^2\ln(\frac{m_R^2}{M_{N\alpha}^2})}{(M_{N\alpha}^2 - m_R^2)^2}\right), \tag{2.22}$$

where the last line is the first order approximation of the small mass difference between m_R^2 and m_I^2; $m_R^2 - m_I^2 = \Delta m^2$.[4] Then the normalized neutrino mass eigenvalues are given in terms of neutrino mass eigenvalues; ${\rm diag}(\tilde m^2_{\nu_1}, \tilde m^2_{\nu_2}, \tilde m^2_{\nu_3}) = {\rm diag}(m^2_{\nu_1}, m^2_{\nu_2}, m^2_{\nu_3})/k_3^2$. It is found that k_3^2 is given by

$$k_3^2 = \frac{\Delta m^2_{\rm atm}}{\tilde m^2_{\nu_3} - \tilde m^2_{\nu_1}}, \tag{2.23}$$

[4]Advantage of this approximation is that $\tilde k_\alpha$ does not depend on Δm.

where normal hierarchy is assumed and $\Delta m^2_{\rm atm}$ is the atmospheric neutrino mass difference square. Comparing Eq. (2.22) and Eq. (2.25), we find Δm^2 is rewritten by the other parameters as follows:

$$\Delta m^2 \approx k_3\left(\frac{M_{N2}[M_{N2}^2 - m_R^2 + M_{N2}^2\ln(\frac{m_R^2}{M_{N2}^2})]}{(M_{N2}^2 - m_R^2)^2}\right)^{-1}. \tag{2.24}$$

The solar neutrino mass difference square is also found as

$$\Delta m^2_{\rm sol} = \Delta m^2_{\rm atm}\frac{\tilde m^2_{\nu_2} - \tilde m^2_{\nu_1}}{\tilde m^2_{\nu_3} - \tilde m^2_{\nu_1}}, \tag{2.25}$$

In numerical analysis, this value should be within the experimental result, while $\Delta m^2_{\rm atm}$ is expected to be input parameter.

DM is expected to be an imaginary component of inert scalar η; η_I. In order to avoid the oblique parameters, we assume to be $m_{\eta^\pm} \approx m_I$ for simplicity. In this case, the mass of DM is uniquely fixed by the observed relic density which suggests it is within 534 ± 8.5 GeV [57], if the Yukawa coupling is not so large. In fact, tiny Yukawa couplings are requested by satisfying the data. Thus, we just work on the mass of η at this narrow range.

III. NUMERICAL ANALYSIS

Here, we show numerical analysis to satisfy all of the constraints that we discussed above, where we work on a basis that the neutrino mass ordering is normal hierarchy.[5] The range of absolute value of the five complex dimensionless parameters α_ν, β_ν, ρ_ν, σ_ν, σ_ℓ are taken to be $[0.01 - 1]$, while the mass parameters M_0, M_1 are of the order [50,500] TeV. We have only two right handed neutrino, therefore $m_1 = 0$ eV and $\alpha_{21} = 0$ [deg].

Figure 1 shows the sum of neutrino masses $\sum m (\equiv {\rm Tr}[D_\nu])$ versus $\sin^2\theta_{12}$ (red color), $\sin^2\theta_{23}$ (blue color) in the left figure, and $\sin^2\theta_{13}$ in the right figure. Here, the horizontal black solid lines are the best fit values, the green dotted lines show 3σ range, and the vertical black line shows upper bound on the cosmological data as shown in the neutrino section. It suggests that all the three mixings run over whole the range of experimental results at 3σ interval, even though larger value of $\sin^2\theta_{23}$ is somewhat favored. While the sum of neutrino masses is restricted to be $\sum m \approx 0.06$ eV that always satisfies the upper bound on the cosmological result.

Figure 2 shows phase of δ^ℓ_{CP} in terms of α_{31}. This figure implies that Dirac CP is linearly proportional to α_{31} phase

[5]We have checked that the inverted hierarchy is not favored in our model.

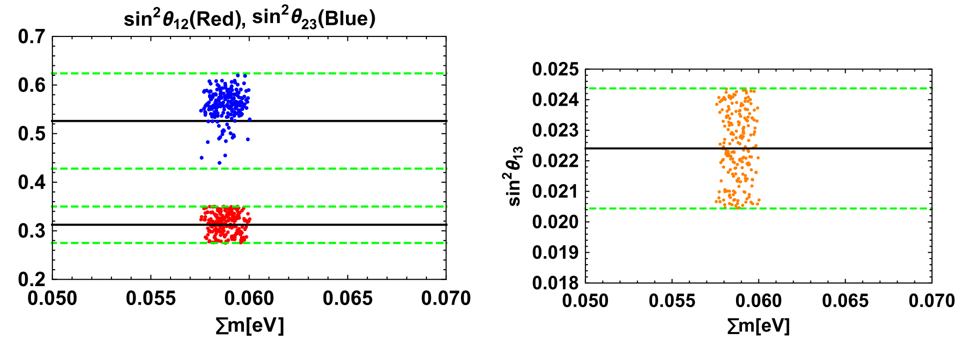

FIG. 1. The sum of neutrino masses $\sum m(\equiv \mathrm{Tr}[D_\nu])$ versus $\sin^2\theta_{12}$ (red color), $\sin^2\theta_{23}$ (blue color) in the left figure, and $\sin^2\theta_{13}$ (orange color) in the right figure. Here, the horizontal black solid lines are the best fit values, the green dotted lines show 3σ range, and the vertical black line shows upper bound on the cosmological data as shown in the neutrino section.

that runs over whole the ranges. Once the Dirac *CP* phase could be fixed to be ~270 [deg] in future experiments, α_{31} is predicted to be ~200 [deg].

Figure 3 demonstrates the sum of neutrino masses versus the effective mass for the neutrinoless double beta decay. It suggests that $0.0035\ \mathrm{eV} \lesssim \langle m_{ee}\rangle \lesssim 0.045\ \mathrm{eV}$. Another remarks are in order:

(1) The typical region of modulus τ is found in narrow space as $-0.1 \lesssim \mathrm{Re}[\tau] \lesssim 0.1$ and $1.2 \lesssim \mathrm{Im}[\tau] \lesssim 1.3$.

(2) Typical scale of LFVs are very small in our analyses, therefore following upper bounds are realized:

$$\mathrm{BR}(\mu \to e\gamma) \lesssim 3.0 \times 10^{-19},$$
$$\mathrm{BR}(\tau \to e\gamma) \lesssim 2.5 \times 10^{-19},$$
$$\mathrm{BR}(\tau \to \mu\gamma) \lesssim 1.5 \times 10^{-20}.$$

(3) The lightest Majorana mass eigenstate is given by [2–9] TeV.

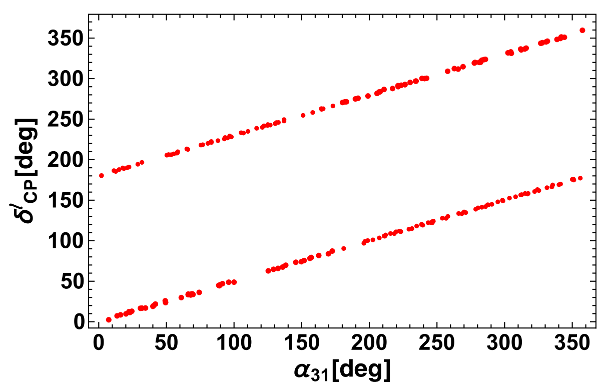

FIG. 2. Phase of δ^{ℓ}_{CP} in terms of α_{31}.

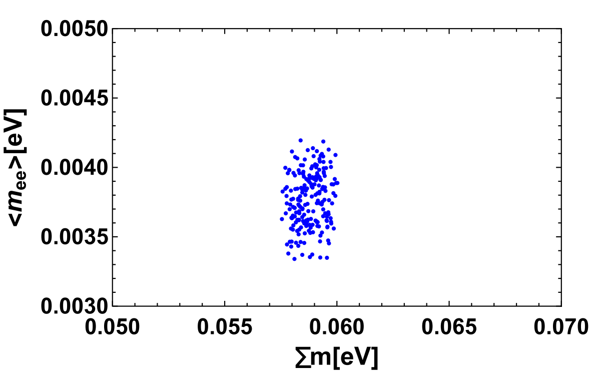

FIG. 3. The sum of neutrino masses versus the effective mass for the neutrinoless double beta decay.

IV. CONCLUSION AND DISCUSSION

We have constructed a predictive lepton model with modular S_3 symmetry in framework of one-loop induced radiative seesaw model. The DM stability is naturally assured by Z_2 symmetry, and DM is correlated with neutrinos in a specific manner, where their interactions are determined by the S_3 symmetry that is known as the minimal group in non-Abelian discrete flavor symmetries. In our numerical analyses, we have highlighted several remarks as follows:

(1) The Dirac phase and the Majorana phase are strongly correlated.

(2) The typical region of modulus τ is found in narrow space as $-0.1 \lesssim \mathrm{Re}[\tau] \lesssim 0.1$ and $1.2 \lesssim \mathrm{Im}[\tau] \lesssim 1.3$.

(3) Typical scale of LFVs are very small in our analyses, therefore following upper bounds are realized:

$$\mathrm{BR}(\mu \to e\gamma) \lesssim 3.0 \times 10^{-19},$$
$$\mathrm{BR}(\tau \to e\gamma) \lesssim 2.5 \times 10^{-19},$$
$$\mathrm{BR}(\tau \to \mu\gamma) \lesssim 1.5 \times 10^{-20}.$$

(4) The lightest Majorana mass eigenstate is given by [2–9] TeV.

ACKNOWLEDGMENTS

This research was supported by an appointment to the JRG Program at the APCTP through the Science and Technology Promotion Fund and Lottery Fund of the

Korean Government. This was also supported by the Korean Local Governments—Gyeongsangbuk-do Province and Pohang City (H. O.). H. O. is sincerely grateful for the KIAS member, and log cabin at POSTECH to provide nice space to come up with this project. Y. O. was supported from European Regional Development Fund-Project Engineering Applications of Microworld Physics (No. CZ.02.1.01/0.0/0.0/16_019/0000766).

[1] E. Ma, Phys. Rev. D **73**, 077301 (2006).
[2] R. de Adelhart Toorop, F. Feruglio, and C. Hagedorn, Nucl. Phys. **B858**, 437 (2012).
[3] F. Feruglio, arXiv:1706.08749.
[4] J. C. Criado and F. Feruglio, SciPost Phys. **5**, 042 (2018).
[5] T. Kobayashi, N. Omoto, Y. Shimizu, K. Takagi, M. Tanimoto, and T. H. Tatsuishi, J. High Energy Phys. 11 (2018) 196.
[6] H. Okada and M. Tanimoto, Phys. Lett. B **791**, 54 (2019).
[7] T. Nomura and H. Okada, Phys. Lett. B **797**, 134799 (2019).
[8] H. Okada and M. Tanimoto, arXiv:1905.13421.
[9] F. J. de Anda, S. F. King, and E. Perdomo, arXiv:1812.05620.
[10] P. P. Novichkov, S. T. Petcov, and M. Tanimoto, Phys. Lett. B **793**, 247 (2019).
[11] T. Nomura and H. Okada, arXiv:1906.03927.
[12] G. J. Ding, S. F. King, and X. G. Liu, J. High Energy Phys. 09 (2019) 074.
[13] H. Okada and Y. Orikasa, arXiv:1907.13520.
[14] T. Nomura, H. Okada, and O. Popov, arXiv:1908.07457.
[15] T. Kobayashi, Y. Shimizu, K. Takagi, M. Tanimoto, and T. H. Tatsuishi, arXiv:1909.05139.
[16] T. Asaka, Y. Heo, T. H. Tatsuishi, and T. Yoshida, arXiv:1909.06520.
[17] G. J. Ding, S. F. King, X. G. Liu, and J. N. Lu, J. High Energy Phys. 12 (2019) 030.
[18] D. Zhang, arXiv:1910.07869.
[19] T. Kobayashi, K. Tanaka, and T. H. Tatsuishi, Phys. Rev. D **98**, 016004 (2018).
[20] T. Kobayashi, Y. Shimizu, K. Takagi, M. Tanimoto, T. H. Tatsuishi, and H. Uchida, Phys. Lett. B **794**, 114 (2019).
[21] T. Kobayashi, Y. Shimizu, K. Takagi, M. Tanimoto, and T. H. Tatsuishi, arXiv:1906.10341.
[22] J. T. Penedo and S. T. Petcov, Nucl. Phys. **B939**, 292 (2019).
[23] P. P. Novichkov, J. T. Penedo, S. T. Petcov, and A. V. Titov, J. High Energy Phys. 04 (2019) 005.
[24] T. Kobayashi, Y. Shimizu, K. Takagi, M. Tanimoto, and T. H. Tatsuishi, arXiv:1907.09141.
[25] S. F. King and Y. L. Zhou, arXiv:1908.02770.
[26] H. Okada and Y. Orikasa, arXiv:1908.08409.
[27] J. C. Criado, F. Feruglio, F. Feruglio, and S. J. D. King, arXiv:1908.11867.
[28] X. Wang and S. Zhou, arXiv:1910.09473.
[29] P. P. Novichkov, J. T. Penedo, S. T. Petcov, and A. V. Titov, J. High Energy Phys. 04 (2019) 174.
[30] G. J. Ding, S. F. King, and X. G. Liu, Phys. Rev. D **100**, 115005 (2019).
[31] A. Baur, H. P. Nilles, A. Trautner, and P. K. S. Vaudrevange, Phys. Lett. B **795**, 7 (2019).
[32] I. de Medeiros Varzielas, S. F. King, and Y. L. Zhou, arXiv:1906.02208.
[33] X. G. Liu and G. J. Ding, J. High Energy Phys. 08 (2019) 134.
[34] G. Altarelli and F. Feruglio, Rev. Mod. Phys. **82**, 2701 (2010).
[35] H. Ishimori, T. Kobayashi, H. Ohki, Y. Shimizu, H. Okada, and M. Tanimoto, Prog. Theor. Phys. Suppl. **183**, 1 (2010).
[36] H. Ishimori, T. Kobayashi, H. Ohki, H. Okada, Y. Shimizu, and M. Tanimoto, Lect. Notes Phys. **858**, 87 (2012).
[37] D. Hernandez and A. Y. Smirnov, Phys. Rev. D **86**, 053014 (2012).
[38] S. F. King and C. Luhn, Rep. Prog. Phys. **76**, 056201 (2013).
[39] S. F. King, A. Merle, S. Morisi, Y. Shimizu, and M. Tanimoto, New J. Phys. **16**, 045018 (2014).
[40] S. F. King, Prog. Part. Nucl. Phys. **94**, 217 (2017).
[41] S. T. Petcov, Eur. Phys. J. C **78**, 709 (2018).
[42] Z. z. Xing, arXiv:1909.09610.
[43] A. Baur, H. P. Nilles, A. Trautner, and P. K. S. Vaudrevange, Nucl. Phys. **B947**, 114737 (2019).
[44] T. Kobayashi, Y. Shimizu, K. Takagi, M. Tanimoto, T. H. Tatsuishi, and H. Uchida, arXiv:1910.11553.
[45] M. Hirsch, S. Morisi, E. Peinado, and J. W. F. Valle, Phys. Rev. D **82**, 116003 (2010).
[46] J. M. Lamprea and E. Peinado, Phys. Rev. D **94**, 055007 (2016).
[47] L. M. G. De La Vega, R. Ferro-Hernandez, and E. Peinado, Phys. Rev. D **99**, 055044 (2019).
[48] P. P. Novichkov, J. T. Penedo, S. T. Petcov, and A. V. Titov, J. High Energy Phys. 07 (2019) 165.
[49] S. Baek, T. Nomura, and H. Okada, Phys. Lett. B **759**, 91 (2016).
[50] M. Lindner, M. Platscher, and F. S. Queiroz, Phys. Rep. **731**, 1 (2018).
[51] A. M. Baldini *et al.* (MEG Collaboration), Eur. Phys. J. C **76**, 434 (2016).
[52] F. Renga (MEG Collaboration), Hyperfine Interact. **239**, 58 (2018).
[53] B. Aubert *et al.* (*BABAR* Collaboration), Phys. Rev. Lett. **104**, 021802 (2010).
[54] N. Aghanim *et al.* (Planck Collaboration), arXiv:1807.06209.
[55] I. Esteban, M. C. Gonzalez-Garcia, A. Hernandez-Cabezudo, M. Maltoni, and T. Schwetz, J. High Energy Phys. 01 (2019) 106.
[56] A. Gando *et al.* (KamLAND-Zen Collaboration), Phys. Rev. Lett. **117**, 082503 (2016); **117**, 109903(E) (2016).
[57] T. Hambye, F.-S. Ling, L. Lopez Honorez, and J. Rocher, J. High Energy Phys. 07 (2009) 090; 05 (2010) 066.